FISEVIER

Contents lists available at ScienceDirect

## Earth and Planetary Science Letters

www.elsevier.com/locate/epsl



## A diatom record of CO<sub>2</sub> decline since the late Miocene



Luz María Mejía <sup>a,b,\*</sup>, Ana Méndez-Vicente <sup>a</sup>, Lorena Abrevaya <sup>a</sup>, Kira T. Lawrence <sup>c</sup>, Caroline Ladlow <sup>c</sup>, Clara Bolton <sup>a,1</sup>, Isabel Cacho <sup>d</sup>, Heather Stoll <sup>a,b,\*</sup>

- a Dept. Geología, Universidad de Oviedo, Arias de Velasco s/n, 33005 Oviedo, Asturias, Spain
- <sup>b</sup> Geological Institute, Department of Earth Science, Sonneggstrasse 5, ETH, 8092, Zürich, Switzerland
- <sup>c</sup> Department of Geology and Environmental Geosciences, Lafayette College, 730 High St, Easton, PA 18042, USA
- d Departament d'Estratigrafia, Paleontologia i Geociències Marines, Universitat de Barcelona, C/Marti i Franquès s/n 28080 Barcelona, Spain

#### ARTICLE INFO

# Article history: Received 31 December 2015 Received in revised form 23 August 2017 Accepted 26 August 2017 Available online xxxx Editor: M. Frank

Keywords:
Miocene
Pliocene
CO<sub>2</sub>
diatoms
carbon isotopes

#### ABSTRACT

Extratropical sea surface temperature records from alkenones record a dramatic cooling of up to 17°C over the last  $\sim$ 14 Ma, but the relationship between this cooling and greenhouse gas forcing has been elusive due to sparse and contrasting reconstructions of atmospheric CO<sub>2</sub> for the time period. Alkenone carbon isotopic fractionation during photosynthesis has previously been used to estimate changes in pCO<sub>2</sub> over this interval, but is complicated by significant changes in cell size of the alkenone-producing coccolithophorids over this time period. In this study, we reconstruct carbon isotopic fractionation during photosynthesis  $(\varepsilon_p)$  using organic compounds trapped within the frustules of pennate diatoms in sediments from the Eastern Equatorial Pacific Ocean at Ocean Drilling Program Site 846 over the last ~13 Ma. Physical separation of pennate diatoms prior to measuring carbon isotopic fractionation enables us to obtain a record with constant cell geometry, eliminating this factor of uncertainty in our pCO<sub>2</sub> reconstruction. In the past  $\sim$ 11 Ma,  $\varepsilon_p$  declines from 15.5 to 10.3%. Using the classic diffusive model and taking into account variations in opal content, alkenone concentration and coccolith Sr/Ca as indicators of past productivity and growth rate, and sea surface temperature records from the site, we estimate a decline in pCO<sub>2</sub> from 454 (+/-41) to 250 (+/-15) ppmv between  $\sim$ 11 and 6 Ma. Models accounting for changing the significance of active carbon uptake for photosynthesis, which likely produce more accurate CO<sub>2</sub> estimates, suggest a significant larger pCO<sub>2</sub> decline of up to twice that shown by the classic diffusive model (in average from 794 (+/-233) ppmv at  $\sim$ 11 Ma to 288 (+/-25) ppmv at  $\sim$ 6 Ma, considering growth rates varying between 0.5 and 1.7 day<sup>-1</sup>). Large uncertainties in the pCO<sub>2</sub> estimated between ~8 and 11 Ma using the active uptake model are related to the growth rate used for calculations. Together, these results suggest CO<sub>2</sub> forcing for this period of steep decline in temperatures. © 2017 Elsevier B.V. All rights reserved.

#### 1. Introduction

The reconstruction of the past partial pressure of atmospheric CO<sub>2</sub> (pCO<sub>2</sub>) is central to assessing climate sensitivity and carbon cycle feedbacks. Because the expected CO<sub>2</sub> concentrations for coming centuries exceed the range recorded in the archive of direct CO<sub>2</sub> determinations from polar ice cores, CO<sub>2</sub> reconstructions of pre-Quaternary periods with warmer temperatures are particularly relevant to the Anthropocene. To date, among an array of different proxies, such as boron isotopes measured in

E-mail addresses: luz.mejia@erdw.ethz.ch (L.M. Mejía),

heather.stoll@erdw.ethz.ch (H. Stoll).

foraminiferal calcite and stomata-based indices, the carbon isotopic fractionation by phytoplankton ( $\varepsilon_p$ ) is the most widely utilized. However, an extensive body of theoretical and experimental studies have documented the dependence of  $\varepsilon_p$  on additional physiological factors such as cell size and growth rate, as well as on CO<sub>2</sub> concentrations (Bidigare et al., 1997; Popp et al., 1998; Rau et al., 1996).

Nearly all previous phytoplankton-based  $\mathrm{CO}_2$  studies have focused on the reconstruction of  $\varepsilon_\mathrm{p}$  from alkenone biomarkers produced by Haptophyte algae. In the fossil record of marine carbonates, Haptophytes are predominantly represented by coccoliths from species belonging to the Nöelaerhabdaceae family. Here, we describe a new record of  $\varepsilon_\mathrm{p}$  determined from the organic matter trapped inside pennate diatom frustules. The physical association of the organic matter with the frustule of the cell producing it allows us to isolate a signal from diatoms of a partic-

<sup>\*</sup> Corresponding authors at: Geological Institute, Department of Earth Science, Sonneggstrasse 5, ETH, 8092, Zürich, Switzerland.

 $<sup>^{\,\,1}\,</sup>$  Present address: Aix-Marseille Université, CNRS, IRD, CEREGE UM34, 13545 Aix en Provence, France.

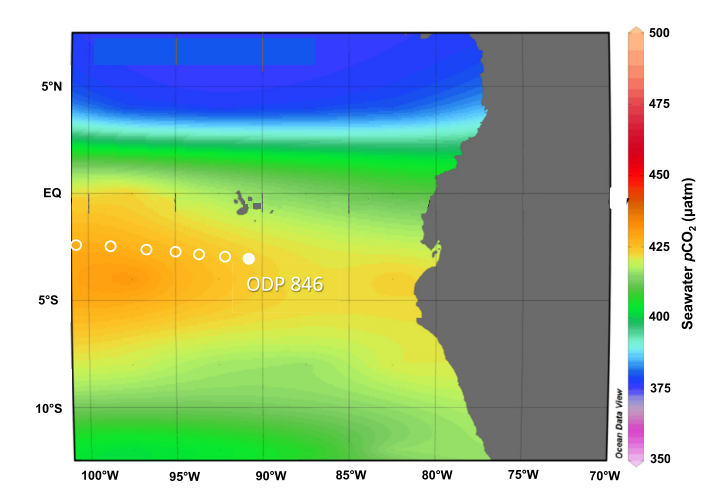


**Fig. 1.** Location of ODP Site 846 over the past 12 Ma (filled circle for modern position; open circles for paleo positions every 2 My) shown over modern partial pressure of CO<sub>2</sub> in seawater (μatm) in the Eastern Equatorial Pacific (EEP) (Takahashi et al. 2015)

ular cell size and geometry, in this case pennate diatoms. Thus, unlike alkenone  $\varepsilon_p$  records, which can be influenced strongly by cell size (Bolton et al., 2016; Henderiks and Pagani, 2008; Seki et al., 2010), diatom  $\varepsilon_p$  records may be produced for a constant cell size over time.

In this study, we use sediments from the Eastern Equatorial Pacific (EEP) Ocean Drilling Program (ODP) Site 846 to produce the first diatom  $\varepsilon_{\rm p}$  record for the late Neogene, spanning the last  $\sim$ 13 Ma. We combine this with independent indicators of primary productivity at this site, based on the abundance of biogenic opal and alkenones, as well as coccolith Sr/Ca, to evaluate the potential influence of growth rate variations on  $\varepsilon_{\rm p}$ . We also introduce a new approach in our pCO<sub>2</sub> estimations that takes into account the variation of CO<sub>2</sub> disequilibrium between the atmosphere and surface waters. Finally, we parametrize active carbon uptake dependent on CO2 supply/demand applying the ACTI-CO model (Bolton and Stoll, 2013) to estimate the effect of modeled active carbon uptake on CO2 estimates. The resulting estimates suggest a trend of declining  $CO_2$  concentrations over the last  $\sim 11$  Ma coinciding with the declining sea surface temperature (SST) (e.g. Herbert et al., 2016; LaRiviere et al., 2012; Rommerskirchen et al., 2011) and  $\delta^{18}$ O trend (Zachos et al., 2008).

#### 2. Site location and oceanographic setting

Over the last  $\sim$ 13 Ma, ODP Site 846 (at 3°05.7′S and 90°49.1′W, depth of 3296 m) has been situated continuously in the upwelling belt of the EEP (Pisias et al., 1995) (Fig. 1), yielding opal rich intervals in the sediments ideal for isolation of diatom frustules for geochemical analysis. Sediments contain alternating nannofossil carbonate and siliceous ooze composed of diatoms and radiolarians (Pisias et al., 1995). Pennate diatoms are dominated by Thalassiothrix longissima, Nitzschia spp., and Thalassionema nitzschioides (Baldauf and Iwai, 1995; Mayer et al., 1992). For diatom geochemistry, we selected samples from local maxima in opal content, from 16 to 45% opal (Farrell et al., 1995), from Hole 846B, spanning a time interval between 0.82 and 12.9 Ma (Appendix A, Table A1). The age model for the last 5.3 Ma is based on correlation of benthic  $\delta^{18}$ O from ODP Site 846 with the "LR04 stack" (Lisiecki and Raymo, 2005), whereas chronology for the older sediments is based on correlation of bulk density (GRAPE) to variations in Northern Hemisphere summer insolation (Shackleton et al., 1995). We seek to capture long term trends with a sample resolution of  $\sim$ 2 My, but avoid the interval of very high productivity centered at  ${\sim}2$  Ma (Lawrence et al., 2006), and instead sample at 0.81 and 3.99 Ma

In the EEP, trade winds drive equatorial divergent upwelling of waters from below the shallow thermocline (from 40 to 100 m) to the surface waters (Farrell et al., 1995). Thus, maximum diatom production associated with upwelling events is mainly restricted to waters depths above 100 m. Subthermocline waters are sourced from the extratropics, predominantly from the Southern Hemisphere through Antarctic intermediate and mode waters (Lawrence et al., 2006). Despite the important oceanographic reorganization associated with the closure of the Panama Isthmus (Sepulchre et al., 2014), the study of Lawrence et al. (2006) suggests that the "plumbing" of the EEP upwelling system has remained relatively constant at least over the last 5 Ma, as high latitudes have regulated EEP surface waters since then, a condition that appears to have been extended even further into the past (Seki et al., 2012). Upwelling in the EEP drives moderately high productivity all year round (average of 100-200 g C m<sup>-2</sup> yr<sup>-1</sup>) (Diester-Haass et al., 2006; Farrell et al., 1995). Due to iron-limitation, upwelled nutrients and DIC are incompletely consumed in the modern surface waters (Behrenfeld et al., 1996) leading to outgassing of CO2 from upwelled waters to the atmosphere (Fig. 1).

#### 3. Materials and methods

# 3.1. Diatom separation, clay removal and non frustule-bound organic matter cleaning

Diatoms were isolated from the <150 µm sediment fraction. Carbonate was dissolved overnight using 5% HCl. Diatom separations were conducted by microfiltration in sodium hexametaphosphate (SHMP), to disaggregate sediments. The carbonate-free sediment was microfiltered at 20 µm to eliminate large centric diatoms, radiolaria and their fragments. The <20 µm fraction was subsequently exhaustively microfiltered at 8 µm, so as to obtain the 0-8 µm size fraction, which is enriched in pennate diatoms with widths <8 µm that pass through the mesh in a vertical orientation. This can be verified in the scanning electron microscope (SEM) images, which show that the length of pennate diatoms composing the 0-8  $\mu$ m size fraction are predominantly >8  $\mu$ m (Fig. 2). Small fragments were eliminated from this pennate diatom fraction by repeated centrifugation in high purity (Milli-Q) deionized distilled water (6 times at 250 rpm for 3 min). For this, we used 15 mL polypropylene tubes filled to 3 mL and subsequently we pipetted and discarded the supernatant rich in fragments. For two samples (0.82 and 12.89 Ma) a 10 µm rather an 8 µm microfilter was employed because the 8 µm filters were unavailable from the supplier during the time of preparation of these samples. For samples in which the pennate contribution to the pennate size fraction was <60% (i.e. samples at 8.86 and 12.89 Ma; Fig. 3g), we have separated the non-pennate fraction, which is mostly composed of centric diatoms and radiolaria (and their fragments) (Appendix A, Table A2), so as to estimate the frustule/diatom bound organic carbon isotopic composition ( $\delta^{13}C_{DB}$ ) and  $\varepsilon_p$  from the pure pennate diatom endmember (Fig. 3a, f). After separation, fractions were dried at 55 °C and stored in teflon tubes.

Samples were observed under the SEM to estimate the percentage of pennate diatom contribution to the total opal of each sample. This was calculated as the fraction of opal composed of pennate diatoms or pennate fragments, relative to the total opal area observed in SEM images. Other size fractions obtained in the course of microfiltration were not employed for further analysis because radiolarian fragments were abundant in the  $>20~\mu m$  size fraction and their elimination in several samples was not possible.

Clay removal from samples consisted of sediment disaggregation via settling in SHMP and separation by density using sodium

### Download English Version:

# https://daneshyari.com/en/article/5779582

Download Persian Version:

https://daneshyari.com/article/5779582

<u>Daneshyari.com</u>